Scientific Drilling (1992) 3:153–160

Scientific Drilling

Anisotropic strength of some typical metamorphic rocks from the KTB pilot hole, Germany

Lev Vernik, David Lockner*, and Mark D. Zoback

Department of Geophysics, Stanford University, Stanford, CA 94305, USA

Summary. Mechanical properties of rocks penetrated by the KTB pilot hole have strong implications for the estimation of in situ stress orientation and magnitude at depth using wellbore breakouts. This study reports on the results of dry triaxial tests of four typical rock types retrieved from the hole and their utilization in constructing models of rock strength anisotropy. The tests were conducted at room temperature and confining pressures from 5 to 75 MPa on 25.4-mm-in-diameter samples cut out at various angles to foliation/lineation (predominantly 30°) and perpendicular to foliation/lineation. Great care was taken to ensure that the samples were devoid of cracks or veins. Rock fabric and post-deformation structures were examined in thin-sections impregnated with blue epoxy. The results indicate major differences in strength and strength anisotropy between the four lithologies with anisotropy varying from 9-12% in lineated amphibolites to 42-60% in mica-rich foliated gneisses. Stress-strain curves of the mica-rich gneisses display features of brittle deformation at low pressure and some elements of brittle-plastic deformation at higher pressures, notably rocks shortened at 30° to foliation. Amphibolites display elastic-brittle behavior over the entire range of applied confining pressures independent of orientation. Modeling of anisotropy based on Coulomb theory proved to be consistent with experimental results.

Introduction

Foliation and lineation in regionally metamorphozed rocks develop as a result of dynamic recrystallization due to superimposed tectonic stress fields and give rise to elastic and mechanical anisotropy. Specifically, the anisotropic mechanical response and strength of gneiss, amphibolite, and schist was documented in several studies (e.g., Borg and Handin 1966; Donath 1972; Gottschalk et al. 1990; Vernik and Zoback 1990). The directional variations in the compressive strength of the rocks tested in those experiments show similar trends with maximal values normal and parallel to the fabric orientation and minimal values at angles of 30° to 45° to it. Gneisses possessing both planar and linear fabric display anisotropy even when shortened in the foliation plane normal and then at an oblique angle to the lineation (Gottschalk et al. 1990).

Understanding these anisotropic properties is critical not only for fault and shear zone mechanics, but also in utilization of a relatively new method of the in situ stress estimation from stress-induced wellbore breakout analysis (e.g., Barton et al. 1988), notably in holes drilled in anisotropic crystalline rock (Vernik and Zoback 1989; Vernik and Zoback 1991). In these studies a methodology was developed for the evaluation of the effective anisotropy defined as the compressive strength variation in the plane normal to the borehole axis. This effective anisotropy was shown to be a function of the maximum strength anisotropy of the rock around the hole and orientation of the rock fabric with respect to the borehole axis.

The problem of effective anisotropy is especially severe in estimating the orientation and magnitude of horizontal stresses based on breakout data in the KTB scientific drilling project (Mastin et al. 1991). The critical question is to what extent the orientation and morphology of wellbore breakouts in anisotropic rock reflect the orientation and magnitude of in situ stresses acting in the drillhole environment. Systematic measurements of the uniaxial compressive and tensile strengths on cores of the KTB hole was undertaken by Rockel and Natau (1990). In compressive tests, a number of 100-mm-in-diameter systematically sampled cores from the pilot hole were axially shortened to failure. The results indicate a dramatic variations in both strength and mechanical anisotropy with depth. These tests supply a valuable information on the rock strength distribution in the well section; however, the following features complicate their utilization for breakout studies: (1) because of the large sampe size, the test results may be strongly affected by natural and drilling-induced fractures; (2) fabric-induced maximum anisotropy is hard to evaluate due to the effects of the dip of foliation (all cylindrical samples were cut parallel to the wellbore, regardless of foliation dip); (3) the internal friction coefficient cannot be estimated.

In this paper we present the results of triaxial tests on carefully selected, crack-free cylindrical samples cut out from the cores representing most typical rock groups in the KTB

* United States Geological Survey, Menlo Park, CA, USA

Offprint requests to: L. Vernik

drillhole section. The primary motivation of this study was to understand the relative roles of strength anisotropy and in situ stress in causing breakouts and further apply the results in estimating the maximum horizontal stress orientation and magnitude.

Experimental Method

The 24 rock cylinders prepared for this study were cored from 5 large sections of cores selected to represent major petrographic rock types in the section of the KTB pilot hole. These rock types included: (1) muscovite-biotite gneiss with various amounts of chlorite and minor amounts of garnet and sillimanite (Mu-Bi Gneiss); (2) biotite gneiss with garnet (Bi Gneiss); (3) hornblende-biotite gneiss with garnet (Hb-Bi Gneiss), and (4) garnet amphibolite (Amphibolite). The difference between Mu-Bi Gneiss and Bi Gneiss is more textural than mineralogical. The former is ubiquitous in the hole and typically has fine- to medium-grained texture with distinct, mm-wide and up to cm-long lenticular segregations of micas aligned with compositional banding and defining the foliation plane in these lithologies. Bi Gneiss is characterized by fine-grained, homogeneous texture with foliation stressed only by a preferred orientation of biotite (001) basal planes. In terms of mineralogy, Bi Gneiss is a more leucocratic rock with 12 to 15% of phyllosilicates (biotite, muscovite, chlorite) compared to Mu-Bi Gneiss which is characterized by about 15 to 20% of the gross amount of these strongly anisotropic minerals.

Hb-Bi Gneiss is encountered only sporadically in the well section and is characterized by a weak preferred orientation of very fine-grained biotite and hornblende, but fairly distinct compositional banding on the mm-scale. The most widespread type of metabasite in the hole is fine- to medium-grained garnet amphibolite with weak linear fabric defined by the elongated shape and crystallographic preferred orientation of the c-axis of hornblende. The lineation in the amphibolites is typically nearly horizontal.

Since the fabric in Mu-Bi Gneiss is predominantly planar, unlike the one described for Four-Mile gneiss by Gottschalk et al. (1990), and the fabric in amphibolite is linear, we have chosen to core cylinders in at least two directions with respect to the fabric orientation. The first direction was normal to foliation or lineation (90°S or 90°L) and the second was at an angle of 30° to it (respectively, 30°S and 30°L). It should be pointed out, however, that in the case of amphibolite there was a considerable ambiguity in determining the coring direction due to the weak, poorly-defined linear fabric of this rock. All cylinders, except those oriented normal to foliation in gneisses, were cored in the plane orthogonal to the core axis, which makes these tests most relevant to wellbore breakout formation. The 30°S direction was suggested by the fact that the shear stress ($|\tau| - \mu\sigma_n$) resolved on planes of this orientation reaches the maximum for the coefficient of internal friction m (0.6 to 1.0) commonly measured in rocks , even though the maximum shear stress is oriented at 45° to the loading axis. Thus by testing a rock in two directions with respect to its predominant fabric element we expected to achieve a better estimate of its maximum strength anisotropy.

The diameter of the cylinders prepared was 25.4 mm and the length-to-diameter ratio was 2 to 2.5. This specimen size is sufficient to contain a large number of constituent mineral grains but small enough to exclude major discontinuities (such veins and drilling-induced fractures), so that the rock possesses gross homogeneous properties (Jaeger and Cook 1979). Also, this size is fairly appropriate in terms of scaling with the dimensions and morphology of wellbore breakouts around a hole with a nominal diameter of 15 to 20 cm.

The dry cylinders were shortened in stiff testing machine with servo-controlled displacement at strain rate of about 10^{-5} sec^{-1}. Mechanical data are reported as differential stress versus axial stain corrected for the piston and contact stiffnesses. Samples were jacketed in tygon tubing and confining pressure applied to approximately correspond to the minimum principal stress acting at the wellbore wall at depths 0.5, 2.5, 3.5, and 7.5 km. This minimum principal stress should be equal to the mud fluid pressure at each specific depth; hence, confining pressures of 5, 25, 35, and 75 MPa were selected for our experiments.

Great care was used in sample selection and cylinder preparation, including optical microscopy and non-destructive ultrasonic sounding. This allowed us to avoid any significant fractures or veins in the test specimens and resulted in good repeatability of experimental results. Repeat tests on 6 cylinders loaded in the same orientation at the same confining pressure showed 2 to 10% strength differences in 5 cases and about 40% difference in one case, possibly due to some microcracks that skipped our attention. This rather low sample-to-sample strength variability makes us confident in further utilizing our test results to estimate mechanical parameters critical for anisotropy modeling in the context of wellbore breakout analysis.

Results and Discussion

Deformation microstructures and stress-strain curves.

The results of all 24 triaxial compression experiments conducted on oriented samples of major petrographic rock types from the KTB pilot hole are given in Table 1. The peak axial stress value σ_{1max} achieved in each test is identified as the rock compressive strength C. Obviously, the C values depend on confining pressure, rock type, and direction of measurements. Overall, the compressive strength at otherwise comparable conditions and orientations is found to increase in the sequence Mu-Bi Gneiss - BiGneiss - Hb-Bi Gneiss - Amphibolite.

Over the entire range of confining pressures, deformation in nearly all experiments was localized within one or more throughgoing shear fractures (Figures 1, 2, 3) with only one exception: a 30°S Mu-Bi Gneiss at 5 MPa failed by formation of a 1.5-cm-thick band stiking parallel to foliation but dipping in the opposite direction. Fractures are throughgoing in other samples of this rock type shortened in the same direction with respect to foliation ; they nucleated and localized within mica-rich segregations parallel to the foliation (Figure 1). In Bi Gneiss shortened at 45°S shear fractures are inclined at lower angles (28° - 29°) to the loading axis and are associated with a well defined zone of axial wing-microcracks (Figure 2). Unlike those in Mu-Bi Gneiss, these shear fractures crosscut foliation planes at oblique angles, even though they strike parallel to the foliation.

Figure 3 shows a typical micrograph of deformation and shear failure in amphibolite shortened at about 25°L to 30°L. The shear fracture is localized within clearly defined 0.2-0.5 mm-thick zone of dense microcracking verging in the same sense as lineation and striking normal to it (Figure 3).

The rightmost column in Table 1 shows fracture dip with respect to the cylinder axis and fracture strike with respect to foliation in gneisses or lineation in amphibolite. The latter

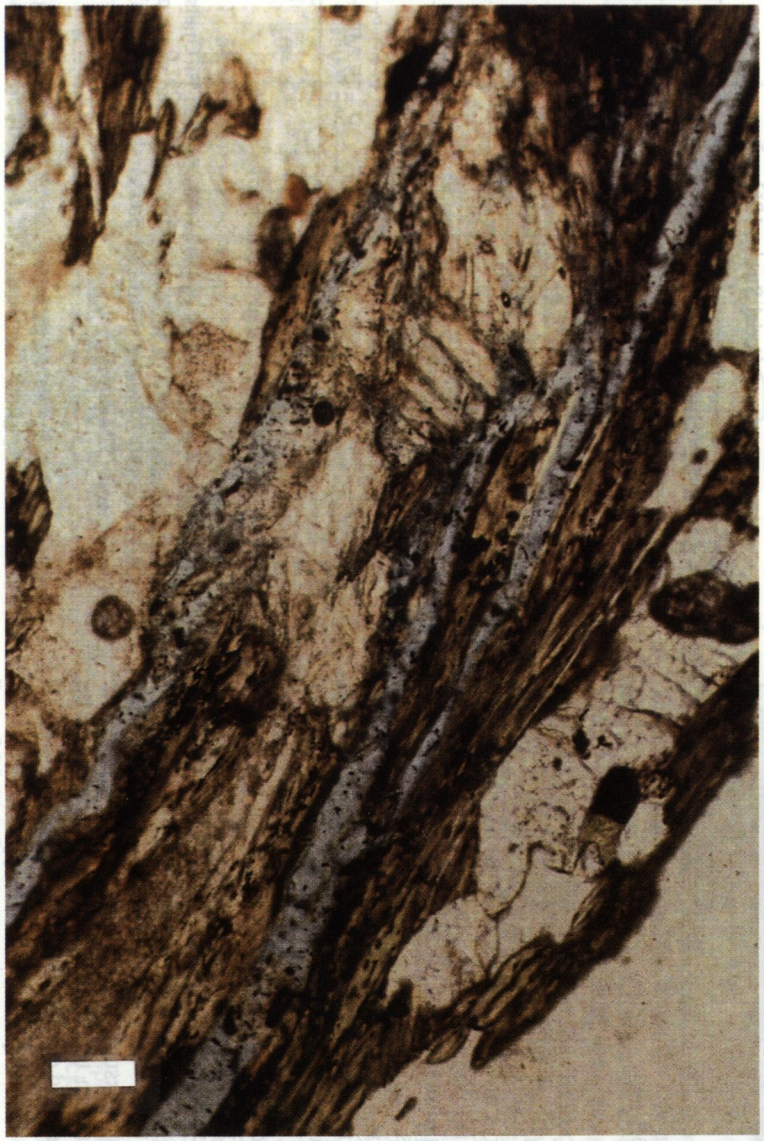

Fig.1. Optical micrographs of shear fractures induced in Mu-Bi Gneiss shortened at 30°S. Throughgoing shear fractures localized in phyllosilicate-reach segregations; scale bar 0.1 mm.

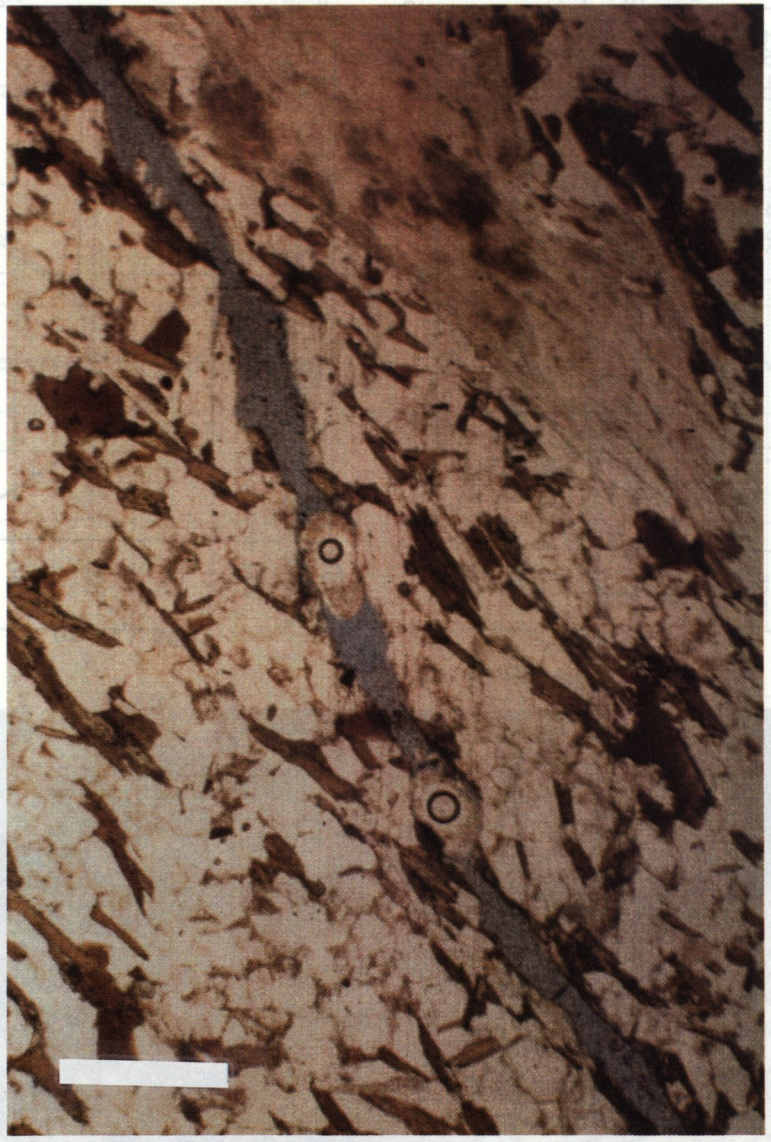

Fig.2. Optical micrograph of shear fracture in Bi Gneiss shortened at 45°S; scale bar 1 mm. Note feather-type axial microcracks associated with the fracture.

Fig.3. Optical micrographs of amphibolite loaded at about 30°L and fractured along well defined shear band of high microcrack density; scale bar 0.1 mm .

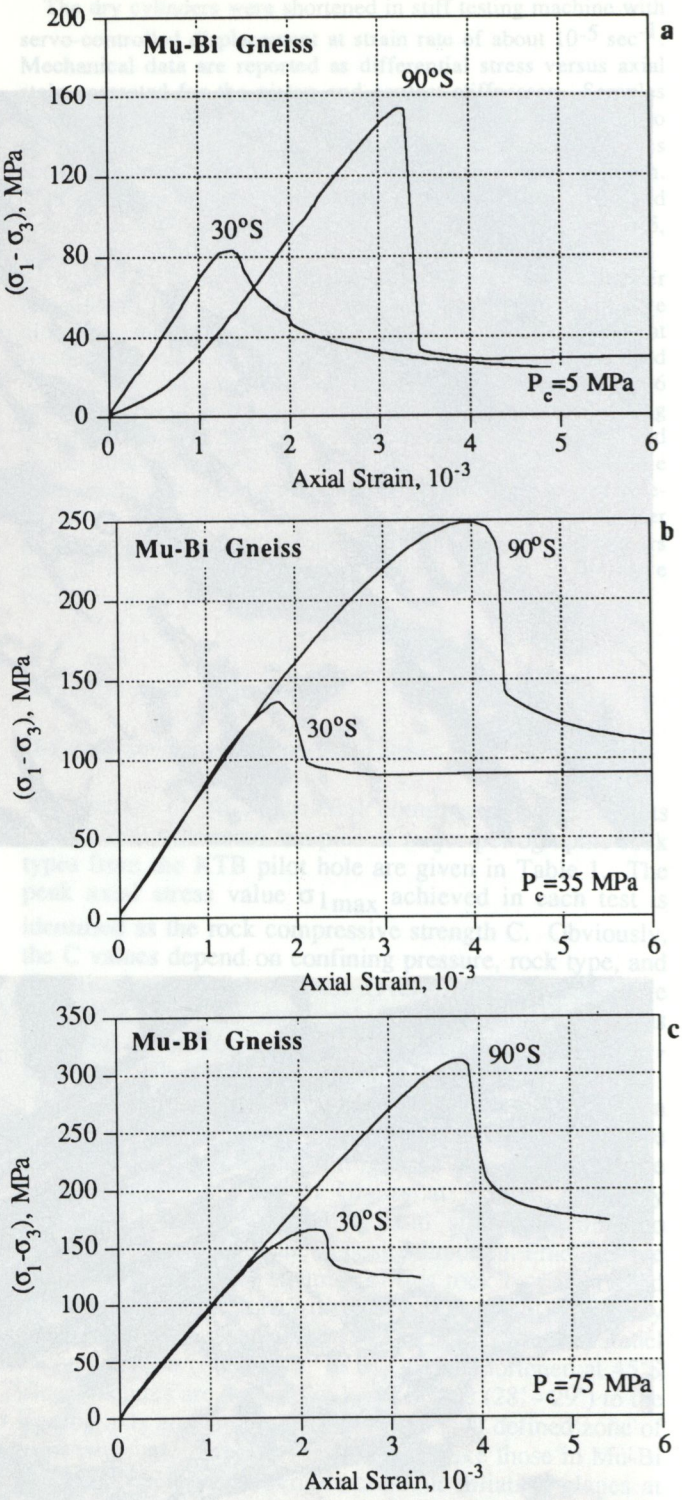

Fig.4. Differential stress - axial strain curves for Mu-Bi Gneiss shortened perpendicularly to foliation (90°S) and at an angle of 30° to foliation (30°S) under confining pressures of 5 MPa (a), 35 MPa (b), and 75 MPa (c).

is not shown for 90°S orientation since it is clear that in this case the fracture strike is always parallel to the foliation. It is most noteworthy that, independent of sample orientation or lithology, the fracture strike is always controlled by foliation plane or lineation direction, whereas the fracture dip is parallel to the foliation only in 30°S Mu-Bi Gneiss. This is a very important observation suggesting that mechanical response of all samples tested at oblique angles to foliation or lineation was influenced by the respective fabric element and the strength variations with angle reflect fabric-induced mechanical anisotropy rather than random sample-to-sample noise.

Typical differential stress versus axial strain curves of samples from the four lithologies are shown in Figures 4 to 7. The curves in these figures are shown in couples for each level of confining pressure; one for oblique and another for orthogonal orientation to fabric so that anisotropy can be visually appreciated and compared for different rock types.

Most dramatic anisotropic behavior is typical of Mu-Bi Gneiss. At low confining pressure (5 MPa) the stress-strain curves corresponding to 30°S and 90°S orientations in this rock differ not only in ultimate peak stress but also in their

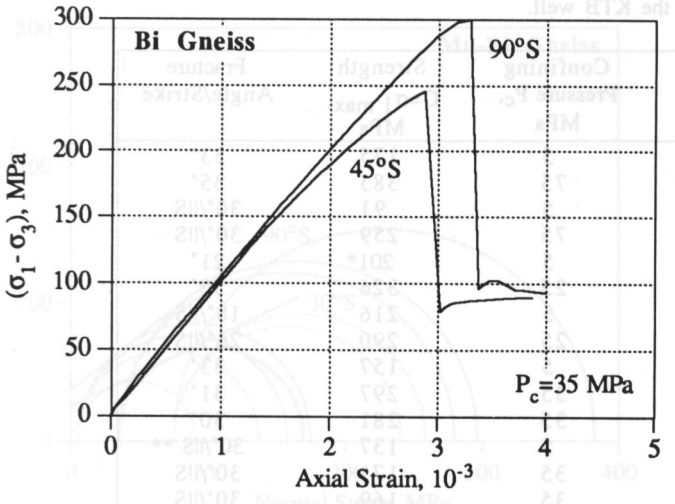

Fig.5. Differential stress - axial strain curves for Bi Gneiss shortened at 90°S and 45°S under confining pressure of 35 MPa.

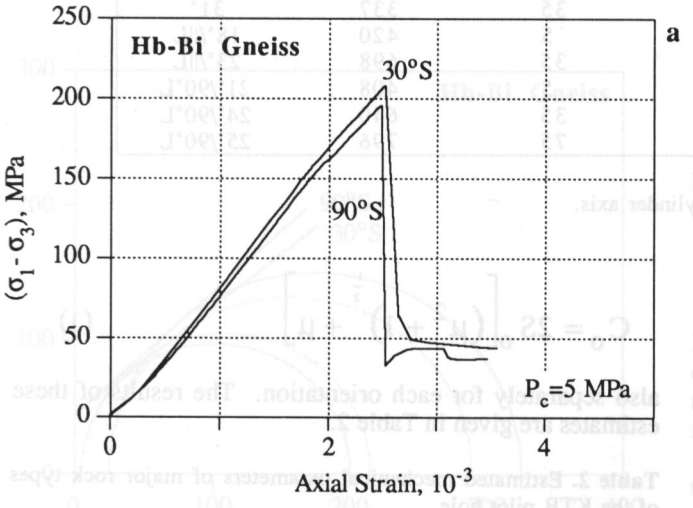

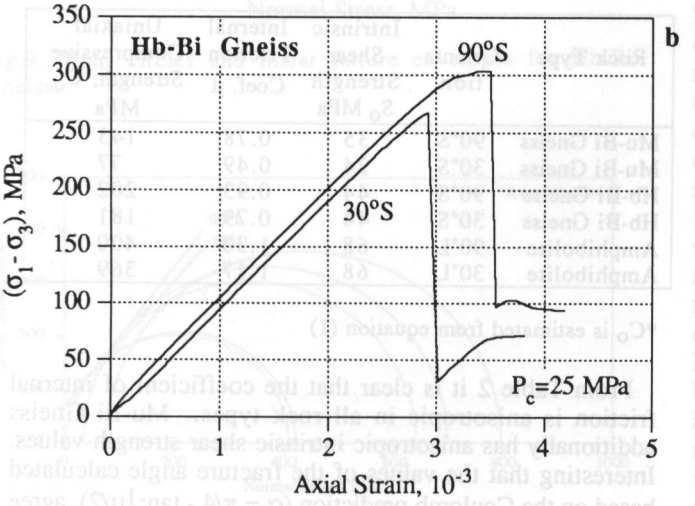

Fig.6. Differential stress - axial strain curves for Hb-Bi Gneiss shortened at 90°S and 30°S under confining pressure of 5 MPa (a) and 25 MPa (b).

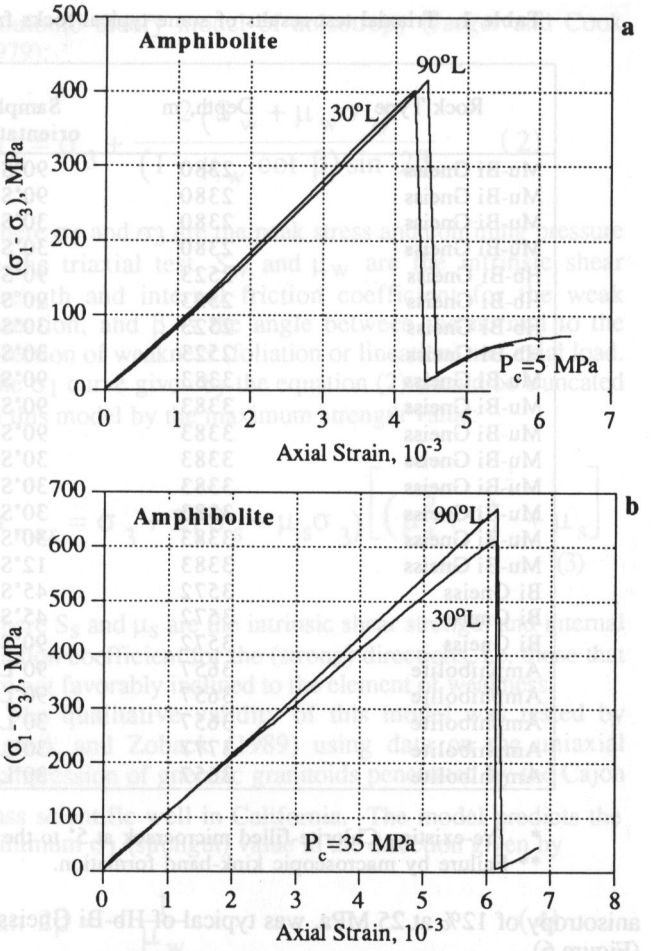

Fig.7. Differential stress - axial strain curves for amphibolite shortened at 90°L and 25°-30°L under confining pressure of 5 MPa (a) and 35 MPa (b).

initial behavior at low differential stress (Figure 4a). Specifically, the 90°S sample displays stress-strain response indicative of the deformation due to microcrack closure, while its 30°S counterpart shows nearly linearly-elastic behavior. This microcrack-induced elastic anisotropy, earlier detected in ultrasonic and static tests in these rocks by Zang et al. (1989) and Rockel and Natau (1990), is controlled by rock mineralogy and fabric and normally introduced into the core samples due to stress relief, thermal cooling, and other processes. These dense, foliation-parallel microcracks in Mu-Bi Gneiss can significantly affect the results of strength anisotropy estimates based on traditional unconfined Brazilian tests. Considering relatively early yielding (at 65-84% of the strength) and post-failure frictional sliding stress levels, we conclude that Mu-Bi Gneiss generally displays features of brittle-plastic behavior, especially obvious at higher confining pressure where the post-failure stress drop was by only 20%.

Even though Bi Gneiss also displayed early deviation from linearity, the failure of this rock was accompanied by significant stress drops independent of orientation (Figure 5). Strength anisotropy in this rock was found to be 23% at P_C = 35 MPa. Similar mechanical response, but with higher yield stress levels (81 to 89% of peak strength) and lower

Table 1. Triaxial test results of some typical rocks from the KTB well.

Rock Type	Depth, m	Sample orientation	Confining Pressure P_C, MPa	Strength $C=\sigma_{1\ max}$, MPa	Fracture Angle/Strike
Mu-Bi Gneiss	2380	90°S	5	175	33°
Mu-Bi Gneiss	2380	90°S	75	383	35°
Mu-Bi Gneiss	2380	30°S	5	91	30°/IIS
Mu-Bi Gneiss	2380	30°S	75	259	30°/IIS
Hb-Bi Gneiss	2523	90°S	5	201*	21°
Hb-Bi Gneiss	2523	90°S	25	326	30°
Hb-Bi Gneiss	2523	30°S	5	216	18°/IIS
Hb-Bi Gneiss	2523	30°S	25	290	26°/IIS
Mu-Bi Gneiss	3383	90°S	5	157	33°
Mu-Bi Gneiss	3383	90°S	35	297	31°
Mu-Bi Gneiss	3383	90°S	35	281	30°
Mu-Bi Gneiss	3383	30°S	5	137	30°/IIS **
Mu-Bi Gneiss	3383	30°S	35	171	30°/IIS
Mu-Bi Gneiss	3383	30°S	35	169	30°/IIS
Mu-Bi Gneiss	3383	30°S	75	241	30°/IIS
Mu-Bi Gneiss	3383	12°S	35	255	25°/IIS
Bi Gneiss	3572	45°S	35	286	29°/IIS
Bi Gneiss	3572	45°S	35	278	28°/IIS
Bi Gneiss	3572	90°S	35	337	31°
Amphibolite	3657	90°L	5	420	18°/IIL
Amphibolite	3657	90°L	35	698	23°/IIL
Amphibolite	3657	30°L	5	408	21°/90°L
Amphibolite	3777	30°L	35	640	24°/90°L
Amphibolite	3657	30°L	75	796	25°/90°L

* Pre-existing Chlorite-filled microcrack at 5° to the cylinder axis.
** Failure by macroscopic kink-band formation.

anisotropy of 12% at 25 MPa, was typical of Hb-Bi Gneiss (Figure 6).

Finally, amphibolite, especially at higher confining pressure showed almost purely linear elastic deformation followed by brittle failure with nearly complete stress drop (Figure 7). Strength anisotropy in amphibolite was only 9% at 35 MPa.

Mechanical parameter estimation and anisotropy modeling.

We have chosen to use simple but straightforward Coulomb failure criterion, $\tau = S_0 + \mu\sigma$, as a first approximation of our experimental results. This criterion is equivalent to the assumption of a linear Mohr envelope. Mohr circles corresponding to our test results are shown in Figures 8, 9, and 10 for Mu-Bi Gneiss, Hb-Bi Gneiss, and amphibolite, respectively. From these figures it is clear that the data cannot be properly fitted by linear envelopes over the entire range of confining pressures from 5 to 75 MPa, and the envelopes should be concave downward. However, as a first order approximation, we have chosen to fit our test results over the range from 5 to 35 MPa, which is of foremost interest for breakout analysis in the KTB pilot hole, by a linear envelope. We make this approximation only for the purpose of estimating the average value of the coefficient of internal friction needed for breakout analysis.

The intrinsic shear strength S_0 and coefficient of internal friction μ are taken as the intercept and slope of the linear Mohr envelope for each orientation in each rock type. The uniaxial compressive strength was calculated as

$$C_o = 2S_o\left[\left(\mu^2+1\right)^{\frac{1}{2}} + \mu\right] \qquad (1)$$

also separately for each orientation. The results of these estimates are given in Table 2.

Table 2. Estimated mechanical parameters of major rock types of the KTB pilot hole.

Rock Type	Orientation	Intrinsic Shear Strength S_0 MPa	Internal Friction Coef. μ	Uniaxial Compressive Strength, C_o MPa
Mu-Bi Gneiss	90°S	35	0.78	143
Mu-Bi Gneiss	30°S	24	0.49	77
Hb-Bi Gneiss	90°S	44	0.93	202
Hb-Bi Gneiss	30°S	44	0.79	181
Amphibolite	90°L	68	1.30	400
Amphibolite	30°L	68	1.17	369

*C_o is estimated from equation (1)

From Table 2 it is clear that the coefficient of internal friction is anisotropic in all rock types. Mu-Bi Gneiss additionally has anisotropic intrinsic shear strength values. Interesting that the values of the fracture angle calculated based on the Coulomb prediction ($\alpha = \pi/4 - \tan^{-1}\mu/2$) agree well with our observations. Even though this should be considered just a coincidence at least in the case of highly anisotropic Mu-Bi Gneiss, the agreement in general gives more confidence in application of the following, based on

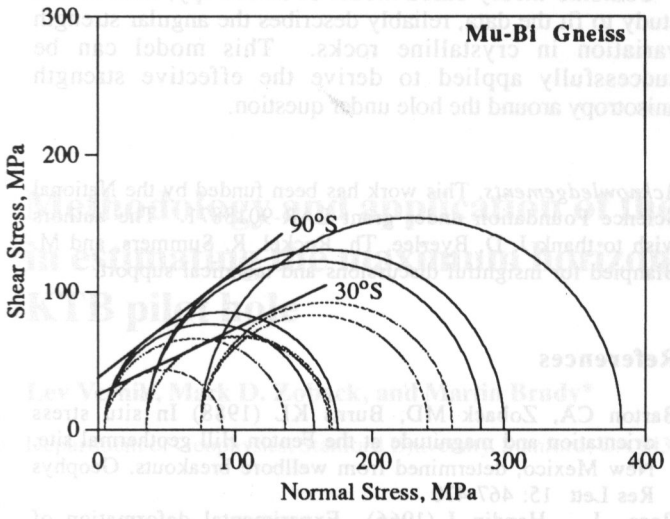

Fig.8. Triaxial test results for Mu-Bi Gneiss presented as Mohr circles separately for 90°S and 30°S orientation. Linear failure envelopes are fitted to the test results at 5 to 35 MPa.

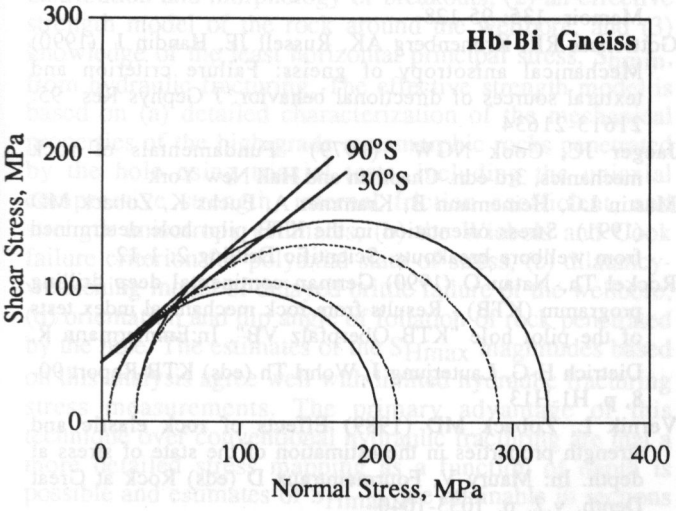

Fig.9. Mohr circles and linear failure envelopes for Hb-Bi Gneiss.

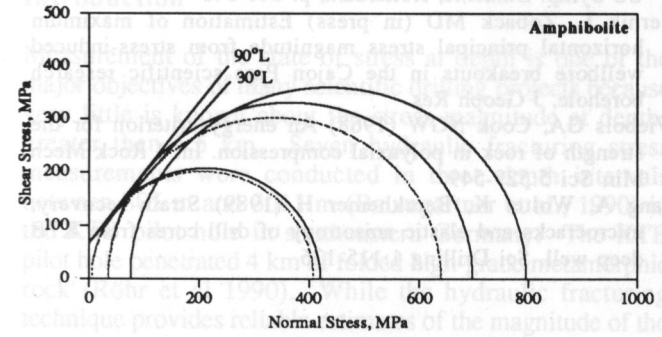

Fig.10. Mohr circles for amphibolite and linear failure envelopes fitted only to the 5 to 35 MPa range of confining pressures.

Coulomb theory model of anisotropy (Jaeger and Cook 1979):

$$\sigma_1 = \sigma_3 + \frac{2(S_w + \mu_w \sigma_3)}{(1 - \mu_w \cot \beta)\sin 2\beta} \qquad (2)$$

where σ_1 and σ_3 are the peak stress and confining pressure in the triaxial test, S_w and μ_w are the intrinsic shear strength and internal friction coefficient for the weak direction, and β is the angle between the normal to the direction of weakness (foliation or lineation) and axial load. The σ_1 curve given by the equation (2) should be truncated in this model by the maximum strength value:

$$\sigma_{max} = \sigma_3 + 2(S_s + \mu_s \sigma_3)\left[(\mu_s^2 + 1)^{\frac{1}{2}} + \mu_s\right] \qquad (3)$$

where S_s and μ_s are the intrinsic shear strength and internal friction coefficient for the (strong) directions, i.e. those that are not favorably inclined to the element of weakness.

The qualitative validity of this model was tested by Vernik and Zoback (1989) using data on the uniaxial compression of gneissic granitoids penetrated by the Cajon Pass scientific well in California. The model predicts the minimum σ_1 (strength) value in the direction given by

$$\tan 2\beta = -\frac{1}{\mu_w} \qquad (4)$$

In our case, when all the input parameters are much better constrained, the model predictions can be taken as quite reliable estimates of strength variation with respect to the fabric direction.

The modeling results are shown in Figure 11 for Mu-Bi Gneiss (a) and amphibolite (b). For Mu-Bi Gneiss the anisotropic model described above fits the data not only for 90°S and 30°S orientations, which were used for parameter derivation, but also for 12°S that can be considered an independent model reliability conformation. The width of the angular range of about 40° of strength reduction compared to the maximum strength of this rock should be emphasized. The error bars indicate about 5% uncertainty in strength based on the repeat tests.

Amphibolite displays a more complicated picture. First, we note that uncertainties exist in this case in both stress and angle-to-lineation measurements due to rather weak fabric associated with elongation and c-axis preferred orientation of fine-grained prisms of hornblende.

Better estimates of the angle are probably somewhere between 25°L and 30°L. If so, the model in Figure 11b indicates that our tests of amphibolite failed to sample the maximal strength anisotropy because the minimum strength values should correspond to about 20°L orientation. This is consistent with the actually observed fracture angles in amphibolite ranging from 18°L to 24°L for low and moderate confining pressures (Figure 2, Table 1). Therefore the 9% strength anisotropy measured at 35 MPa in amphibolite can be taken as a lower bound value. The model in Figure 10b under the same conditions predicts about 12%

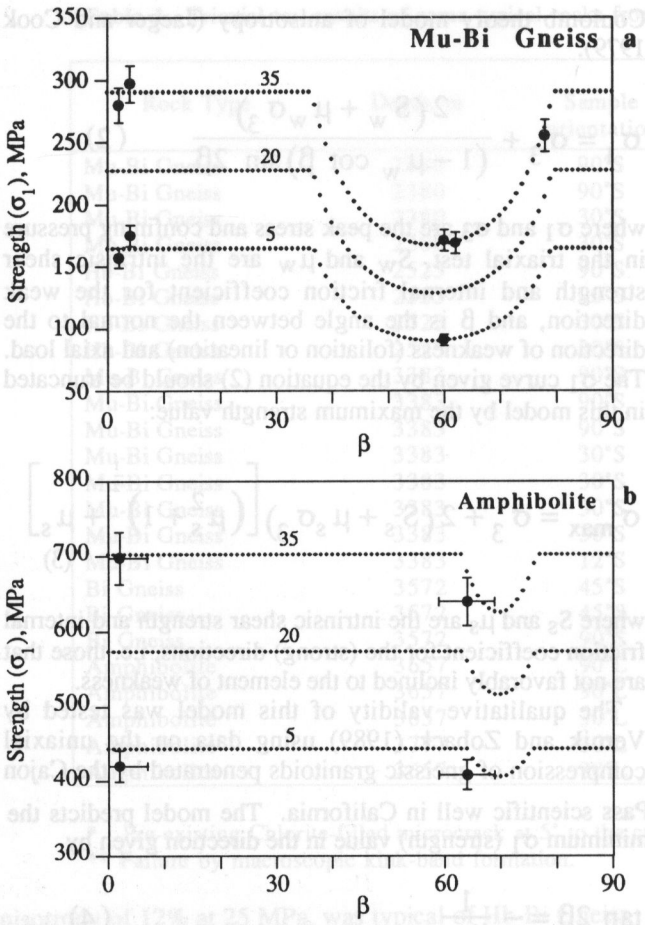

Fig.11. Strength anisotropy models based on Coulomb theory with input parameters estimated using linear Mohr envelopes for a range of confining pressure from 5 to 35 MPa for Mu-Bi Gneiss (a) and amphibolite (b). Peak axial stress (strength) is shown as a function of the angle between the compression direction and the normal to foliation in gneiss and lineation in amphibolite.

microcracks that originated due to the slip on favorably oriented biotite flakes similar to that on favorably oriented microcracks in dilated granite (Brace et al. 1966; Gottschalk et al. 1990) with shear fracture obliquely cutting across foliation. In contrast the failure of coarser-grained Mu-Bi Gneiss with foliation-controlled biotite segregations shorted at 30°S always occurred along the foliation, i.e. similar to the failure of slate or phyllite (Borg and Handin 1966; Donath 1972). This difference in deformation micromechanics resulted in more than a factor of 2 difference in strength anisotropy between these two typical rock types from the KTB hole.

Our results indicate that even the least anisotropic rock in the KTB hole, such as amphibolite and Hb-Bi Gneiss, the strength anisotropy is no less than about 9 to 12% and should be taken into account in breakout analysis for stress evaluation. One should also note that since the mechanical anisotropy in amphibolite is due to linear fabric which is normally subhorizontal, the effective anisotropy in this rock will not be reduced as it occurs in gneisses due to the variation in the foliation dip angle (Vernik and Zoback 1989).

Coulomb theory based model of anisotropy, used in this study to fit the data, reliably describes the angular strength variation in crystalline rocks. This model can be successfully applied to derive the effective strength anisotropy around the hole under question.

Acknowledgements. This work has been funded by the National Science Foundation under grant EAR-9018871. The authors wish to thank J. D. Byerlee, Th. Rockel, R. Summers, and M. Blanpied for insightful discussions and technical support.

References

Barton CA, Zoback MD, Burns KL (1988) In situ stress orientation and magnitude at the Fenton Hill geothermal site, New Mexico, determined from wellbore breakouts. Geophys Res Lett 15: 467-470

Borg I, Handin J (1966) Experimental deformation of crystalline rocks. Tectonophysics 3: 249-368

Brace WF, Paulding BW, Scholz C (1966) Dilatancy in the fracture of crystalline rocks. J Geophys Res 71: 3939-3953

Donath FA, (1972) Effects of cohesion and granularity on deformation behavior of anisotropic rock. Geol Soc Amer Memoir 135: 95-128

Gottschalk RR, Kronenberg AK, Russell JE, Handin J (1990) Mechanical anisotropy of gneiss: Failure criterion and textural sources of directional behavior. J Gephys Res 95: 21613-21634

Jaeger JC, Cook NGW (1979) Fundamentals of rock mechanics, 3rd edn. Chapman and Hall New York

Mastin LG, Heinemann B, Krammer A, Fuchs K, Zoback MD (1991) Stress orientation in the KTB pilot hole determined from wellbore breakouts. Scientific Drilling 2: 1-12

Rockel Th, Natau O (1990) German continental deep drilling programm (KTB) - Results from rock mechanical index tests of the pilot hole "KTB Oberpfalz VB". In:Emmermann R, Dietrich H-G, Lauterjung J, Wohrl Th (eds) KTB Report 90-8, p. H1-H13

Vernik L, Zoback MD (1989) Effects of rock elastic and strength properties in the estimation of the state of stress at depth. In: Maury V, Fourmaintraux D (eds) Rock at Great Depth, v.2. p. 1033-1040

Vernik L, Zoback MD (1990) Strength anisotropy in crystalline rock: Implications for assessments of in situ stress from wellbore breakouts. In: Hustrulid WA, Johnson GA (eds) Rock Mechanics Contributions and Challenges; Proc 31st US Symp. Balkema, Rotterdam, p. 841-848

Vernik L, Zoback MD (in press) Estimation of maximum horizontal principal stress magnitude from stress-induced wellbore breakouts in the Cajon Pass scientific research borehole. J Geoph Res

Wiebols GA, Cook NGW (1968) An energy criterion for the strength of rock in polyaxial compression. Int J Rock Mech Min Sci 5:529-549

Zang A, Wolter K, Berckhemer H (1989) Strain recovery, microcracks and elastic anisotropy of drill cores from KTB deep well. Sci Drilling 1:115-126